Radiotherapy and Oncology 130 (2019) 180–184

Contents lists available at ScienceDirect

Radiotherapy and Oncology

journal homepage: www.thegreenjournal.com

High-resolution FLAIR MRI at 7 Tesla for treatment planning in glioblastoma patients

Sebastian Regnery [a,b], Benjamin R. Knowles [c], Daniel Paech [d], Nicolas Behl [c], Jan-Eric Meissner [c], Paul Windisch [a], Semi Ben Harrabi [a,b,f,g], Denise Bernhardt [a,b], Heinz-Peter Schlemmer [d], Mark E. Ladd [c,e], Stefan Rieken [a,b], Jürgen Debus [a,b,f,g], Sebastian Adeberg [a,b,f,g,*]

[a] Department of Radiation Oncology, Heidelberg University Hospital; [b] Clinical Cooperation Unit Radiation Oncology, German Cancer Research Center (DKFZ); [c] Division of Medical Physics in Radiology, German Cancer Research Center (DKFZ); [d] Division of Radiology, German Cancer Research Center (DKFZ), Heidelberg; [e] Faculty of Physics and Astronomy and Faculty of Medicine, University of Heidelberg; [f] Heidelberg Institute of Radiation Oncology (HIRO), Heidelberg; and [g] Heidelberg Ion-Beam Therapy Center (HIT), Im Neuenheimer Feld 450, 69120 Heidelberg, Germany

ARTICLE INFO

Article history:
Received 28 May 2018
Received in revised form 10 July 2018
Accepted 17 August 2018
Available online 31 August 2018

Keywords:
MR-guided radiotherapy
Ultra-High-Field MRI
Glioblastoma

ABSTRACT

Ultra-high field MRI is an emerging technique promising high-resolution images for radiotherapy planning. We compared a 7 Tesla FLAIR sequence with clinical FLAIR imaging at 3 Tesla in glioblastoma patients before radiotherapy. High-resolution 7 Tesla FLAIR imaging may enhance the depiction of organs at risk and possibly modify target volumes.

Currently, MRI at field strengths of up to 3 Tesla (T), based on T1-weighted contrast-enhanced and T2-weighted Fluid-attenuated Inversion Recovery (FLAIR) imaging [1,2], is a cornerstone in the diagnosis and treatment planning of glioblastoma (GBM) [2–4]. Despite greatest-possible resection and adjuvant chemoradiotherapy (CRT), patients still face a poor prognosis [5,6]. A major problem is the aggressive and diffuse infiltration of GBM, particularly along white matter tracts, which often remains invisible on clinical imaging [7–10]. Ultra-high field MRI at field strengths of 7T and above is an emerging imaging technique which yields increased signal-to-noise-ratio (SNR) and allows for higher spatial resolution [11–14]. Specifically, 7T MRI has the potential to depict small anatomical substructures [13,15] and improve diagnostic confidence in the brain [16]. Furthermore, integration of 7T MRI in treatment planning for brain tumors is technically feasible [17]. Hence, 7T MRI might enhance visualization of GBM infiltration as related to neighboring tissues and organs at risk (OARs), thus refining current radiation target volume delineation.

In this preparatory work, we compared clinical FLAIR MRI at 3T with a high-resolution FLAIR sequence at 7T for radiotherapy planning of GBM patients. We hypothesized that the 7T FLAIR sequence would yield higher spatial resolution at equally high image quality, thus providing altered gross-tumor-volumes (GTV).

Patients & methods

Between May 2017 and April 2018, 19 prospective patients consecutively underwent FLAIR imaging at a 7T MRI scanner before CRT. 7T MRI inclusion criteria were age >18 years, eligibility for a 7T MRI examination, histopathological diagnosis of GBM and residual tumor as visible on clinical imaging. Finally, consistent clinical 3T FLAIR MRI was mandatory, so that 15 patients were eligible for this analysis (Table 1).

High-resolution FLAIR imaging was performed on a 7T MRI scanner (MAGNETOM 7.0 Tesla, Siemens Healthineers, Erlangen, Germany) with a single channel transmit/24 channel receive head coil (Nova Medical, Wilmington, USA). Additionally, dielectric pads were used [18]. The sequence based on a Hyperecho approach [19,20] which facilitated adherence to SAR limits [refocusing flip angle: 60°, echo train length: 13, TE: 111 ms, TR: 16000 ms, TI: 3100 ms, 0.57x0.57 mm^2, slice thickness: 5 mm, number of slices: 15, distance factor: 10%]. Sequence duration was 7:30 minutes. After examination, patients were interviewed for possible MRI side effects.

Clinical FLAIR images were obtained on 3T MRI scanners (MAGNETOM Skyra (TrioTIM or Verio), Siemens Healthineers, Erlangen,

* Corresponding author at: Heidelberg University Hospital, Im Neuenheimer Feld 400, 69120 Heidelberg, Germany.
E-mail address: sebastian.adeberg@med.uni-heidelberg.de (S. Adeberg).

https://doi.org/10.1016/j.radonc.2018.08.002
0167-8140/

Table 1
Patient characteristics and data analysis (n = 15). All p-values were additionally adjusted (adj) according to the Bonferroni-Holm method. (CRT = chemoradiotherapy, T = Tesla, FLAIR = fluid-attenuated-inversion-recovery, SNR = signal-to-noise-ratio, SNR_{corr} = corrected signal-to-noise-ratio, WM = white matter, GM = gray matter, PE = peritumoral edema, GTV = gross tumor volume).

Whole Patient group (n = 15)			
Age	[Years]		
Median Age	60		
Interquartile Range	53–66		
Gender	*N*	[%]	
Male	8	53.3	
Female	7	46.7	
Previous Therapy	*N*	[%]	
Biopsy only	4	26.7	
Partial Resection only	6	40.0	
Resection & CRT	5	33.3	
Time span of 3T to 7T FLAIR	[days]		
Median Time Span	7		
Interquartile Range	1–15		
SNR in WM	3T FLAIR	7T FLAIR	*p*-Value (adj)
Median	68.7	48.7	0.2293 (0.2293)
Interquartile Range	37.4–76.7	34.7–72.2	
SNR_{corr} in WM	3T FLAIR	7T FLAIR	*p*-Value (adj)
Median	68.7	107.7	0.0103 **(0.0312)**
Interquartile Range	37.4–76.69	73.8–152.3	
$SNR_{GM/WM}$ ratio	3T FLAIR	7T FLAIR	*p*-Value (adj)
Median	1.14	1.30	0.0103 **(0.0312)**
Interquartile Range	(1.11–1.21)	(1.20–1.38)	
$SNR_{PE/WM}$ ratio	3T FLAIR	7T FLAIR	*p*-Value (adj)
Median	1.85	1.44	0.0004 **(0.002)**
Interquartile range	(1.66–2.03)	(1.28–1.50)	
Subgroup for GTV comparison (N = 8)			
Tumor localization	*N*	[%]	
Frontal	3	37.5	
Frontoparietal	2	25.0	
Frontotemporal	2	25.0	
Parieto-temporal	1	12.5	
GTV	3T FLAIR [ccm]	7T FLAIR [ccm]	
Median	79.09	76.58	
Interquartile Range	21.2–113.7	20.9–90.9	
GTV difference	[% of GTV at 3T]	*p*-Value (adj)	
Median of Differences	−7.4%	0.0078 **(0.0312)**	
Interquartile Range	−3.2% to −11.6%		

Bold values indicate significant *p*-values after Bonferroni-Holm adjustment.

Germany) with 16-channel receive head coils (Siemens Healthineers, Erlangen, Germany) at the same institution after application of a Gadolinium-based contrast agent. All protocols based on a turbo spin echo (TSE) sequence [flip angle: 150° (170°), echo train length: 18 (21), TE: 117 (135)ms, TR: 8500 ms, TI: 2500 (2400)ms, in-plane resolution: $0.74 \times 0.74\ mm^2$ ($0.89 \times 0.89\ mm^2$), slice thickness: 5 mm (4–6 mm), number of slices: adapted to whole head, distance factor: 5%]. Furthermore, pre- and postcontrast T1-weighted imaging was performed [TE: 4.04 ms; TR: 1710 ms; in-plane resolution: $0.25 \times 0.25\ mm^2$; slice thickness: 1 mm].

Corresponding 3T and 7T MR-images were coregistered by employing an automatic multi-modal rigid registration algorithm in MITK [21]. Regions of interest (ROIs) were placed into white matter (WM), adjacent gray matter (GM) and adjacent peritumoral edema (PE) by a radiation oncologist (SA), based on the 3T MRI. PE was defined as FLAIR hyperintensity without enhancement in postcontrast T1-weighted sequences. Additionally, a large ROI was drawn into background noise outside of the skull. SNR values of WM, GM and PE were calculated dividing the mean signal of the corresponding ROI by the mean signal of the background ROI. SNR ratios of GM and WM ($SNR_{GM/WM}$) as well as PE and WM ($SNR_{PE/WM}$) were calculated to evaluate relative image contrast. Finally, a linear normalization of SNR in WM to the voxel size of the 3T sequence was performed to yield a spatial resolution corrected SNR (SNR_{corr}) in WM.

An experienced radiation oncologist (SA) delineated the FLAIR-GTVs using Oncentra External Beam Version 4.5® (Elekta, Sweden). The FLAIR-GTV was defined as the resection cavity plus the whole region of FLAIR abnormality which accounts for the major part of the base plan (=GTV1) according to RTOG (resection cavity plus enhancing lesions plus non-enhancing T2-weighted FLAIR abnormalities) [2]. The corresponding 3T and 7T FLAIR-GTVs were compared in all patients where the whole tumor was covered by the 7T FLAIR imaging and the time span between 3T and 7T MRI was at most 7 days. Consequently, eight patients were eligible.

Median and interquartile range (IQR) of SNR values in WM, the SNR ratios and FLAIR-GTV were calculated for both field strengths. The assessment of differences in SNR in WM, SNR ratios and FLAIR-GTV between the two field strengths employed two-sided Wilcoxon signed-rank tests. The level of statistical significance was set to $\alpha \leq 0.05$ and all *p*-values were adjusted according to the Bonferroni-Holm method to control the family-wise error rate. The statistical analysis was implemented in R version 3.4.3.

This study received approval by the local ethics committee (vote specification: S-343/2016) and written informed consent was obtained from all patients before MRI according to the declaration of Helsinki.

Results

Image quality

FLAIR imaging at 7T yielded a higher spatial resolution without significant reduction in the SNR in white matter (WM) compared to 3T MRI (median SNR in WM at 3T = 68.7 (37.4–76.7), median SNR in WM at 7T = 48.7 (34.7–72.2), adjusted $p = 0.23$). Accordingly, the SNR in WM at 7T reached significantly higher values after normalization to the clinical voxel size (median SNR_{corr} at 3T = 68.7 (37.4–76.7), median SNR_{corr} at 7T = 107.7 (73.8 – 152.3), adjusted $p = 0.03$). As a result, major WM tracts were depicted in more detail in 7T FLAIR images (Fig. 1). Furthermore, the $SNR_{GM/WM}$ ratio was significantly increased at 7T (median $SNR_{GM/WM}$ at 3T = 1.14 (1.11 – 1.21), median $SNR_{GM/WM}$ at 7T = 1.30 (1.20–1.38), adjusted $p = 0.03$). Thus, images showed a better contrast between gray matter (GM) and WM (Fig. 1). Conversely, the relative contrast between peritumoral edema (PE) and WM as represented by the $SNR_{PE/WM}$ ratio showed significantly higher values in the clinical FLAIR imaging (median $SNR_{PE/WM}$ at 3T = 1.85 (1.66–2.03), median $SNR_{PE/WM}$ at 7T = 1.44 (1.28–1.50), adjusted $p = 0.002$).

FLAIR-GTV

Comparison of FLAIR-GTVs between the 3T and 7T imaging showed significantly lower volumes in the 7T FLAIR imaging (median deviation of 7T from 3T = −7.4% (−3.2% to −11.6%), adjusted $p = 0.03$) (Fig. 1).

Side effects

Only two patients complained about one mild side effect (claustrophobia, vertigo) during 7T MRI without the necessity to cancel the examination.

Discussion

In this work, 15 prospective GBM patients underwent high-resolution 7T FLAIR MRI for radiotherapeutic target volume delineation in addition to clinical 3T MRI. The 7T FLAIR yielded significantly higher SNR in WM and contrast between GM and WM, whereas the contrast between PE and WM was significantly decreased. Furthermore, the 7T FLAIR-GTVs were significantly smaller ($N = 8$).

The increase in SNR or rather spatial resolution might enhance anatomical depiction of WM tracts, which are preferred infiltration routes of GBM [9]. Hence, 7T FLAIR could enhance the inclusion of neighboring WM tracts into radiotherapy plans following previous

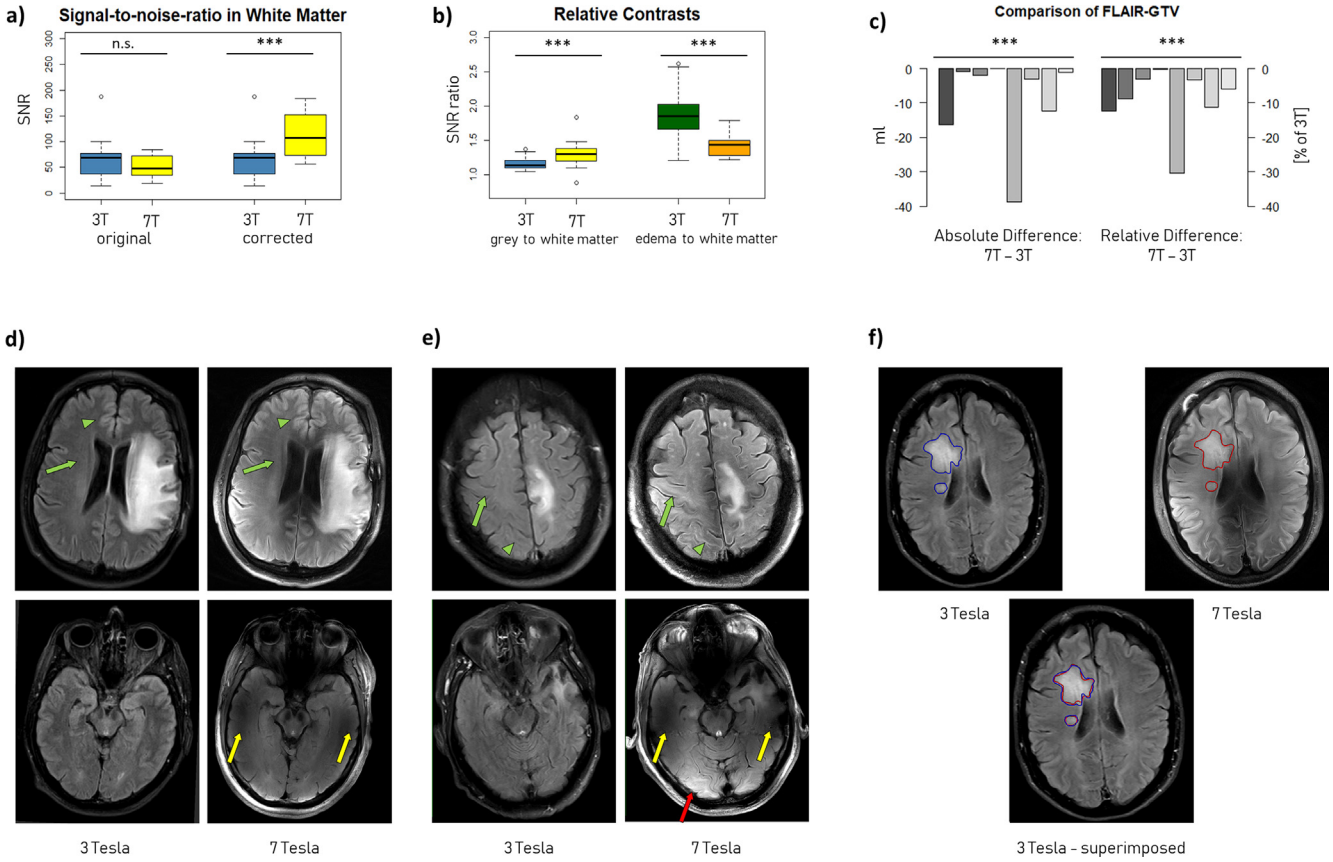

Fig. 1. Comparison of signal-to-noise-ratio (SNR) (a), SNR ratios (b) and gross tumor volume (GTV) (c) between the two different field strengths (*** = statistically significant with $p \leq 0.05$, n.s. = not statistically significant). (a) The corrected SNR is significantly increased at 7T. (b) The relative contrast between white matter (WM) and gray matter (GM) is significantly higher at 7T. But the relative contrast between WM and peritumoral edema (PE) was significantly decreased at 7T. (c) GTVs were smaller at 7T in all observed patients (corresponding patients are shown in the same shade of gray). (d) & (e) Exemplary high-resolution FLAIR MRI at 7T with corresponding clinical MRI at 3T in two patients. The visibility of major WM-tracts (green arrows) and boundaries between GM and WM (green arrowheads) is enhanced in the 7T FLAIR. Near the skull base, artifacts due to signal loss (yellow arrows) and brightening (red arrow) decrease SNR and contrast of the 7T MRI. (f) Exemplary delineation of FLAIR-GTVs at 3T (blue) and 7T (red) with superimposition of the corresponding volumes on the clinical 3T MR-image.

studies employing clinical FLAIR [22]. Additionally, the elevated contrast between GM and WM suggests better visibility of anatomical borders. Therefore, 7T FLAIR could improve the delineation of complex organs at risk such as the hippocampus [15,16], which might be an important structure concerning long-term cognitive impairment [23]. Furthermore, smaller FLAIR-GTVs result in smaller base plans (=GTV1) and possibly disproportionately smaller clinical target volumes (CTV1) according to RTOG [2]. Presently, the EORTC guidelines do not include FLAIR hyperintensities into GTV, but an adaption of the CTV to encompass all FLAIR hyperintensities is discussed especially in secondary GBM [2]. In that case, smaller FLAIR-GTVs would also translate to smaller adapted CTVs. Consequently, altered FLAIR-GTVs in GBM suggest analogous changes in lower-grade gliomas, which would directly affect GTVs and CTVs [24,25]. Possible advantages of more focused CTVs at 7T include improved sparing of OARs as well as enhanced dose coverage of the target volumes but require validation in forthcoming trials.

The imaging duration of 7:30 min as well as the low number of side effects rendered 7T MRI clinically feasible in accordance with previous studies [17,26].

The gain in SNR or rather spatial resolution at 7T is in accordance to previous 7T MRI studies [13,16], although SNR_{corr} of WM increased somewhat less in our work than reported by Zwanenburg et al. [13]. This might be due to examination of physically impaired GBM patients instead of healthy volunteers. Moreover, tumor-related changes could have affected the signals from adjacent normal-appearing tissues. Additionally, the contrast agent applied prior to the 3T FLAIR imaging may have produced an increase in SNR in clinical MRI.

Concerning the contrast between WM and GM, Zwanenburg et al. [13] reported a slight decrease at 7T compared to 3T, whereas the contrasts differed based on the employed sequence in a previous study by Springer et al. [16]. Our findings show a significant increase of the $SNR_{GM/WM}$ at 7T for a Hyperecho-based FLAIR. It may be inferred that the underlying sequence technique has an important impact on image contrast. Moreover, the use of contrast agent with the 3T FLAIR in our study is expected to provide a small increase in WM-GM contrast. Consequently, the native FLAIR contrast difference between 3T and 7T could be even larger than our findings suggest.

Previous studies of current 7T FLAIR MRI applications reported a limiting loss of signal and contrast near the skull base [13,16,17], which was also present within the temporal lobes in our images. This might impede visibility of OARs and GTVs.

The relative contrast between peritumoral edema (PE) and WM, as reflected by the $SNR_{PE/WM}$, was significantly lower in the 7T FLAIR MRI than in clinical FLAIR imaging. Additionally, the 7T sequence yielded consistently smaller FLAIR-GTVs. Those two findings might be connected because $SNR_{PE/WM}$ was measured in the outer rim of PE adjacent to WM, which is the area where FLAIR-GTVs were delineated. Notably, all PE ROIs were defined on 3T MRI. Hence, one could speculate that $SNR_{PE/WM}$ is decreased because FLAIR imaging at 7T provides different signals in peritumoral edema compared to clinical MRI. Possibly, edema borders are relocated on 7T FLAIR MRI, which could provide different information on tumor infiltration and altered tumor volumes. A complementary depiction of tumor infiltration might also support the decision whether FLAIR hyperintensities should be included into a CTV. However, the possible influence of contrast agent on $SNR_{PE/WM}$ in the 3T MRI must be considered, although we carefully excluded all areas of Gadolinium-contrast enhancement as visible on T1-weighted MRI from PE ROIs. Concerning the difference in GTV, other possible influence factors include the lower image quality in the temporal lobes at 7T which might have impeded visibility of tumor edema, but only three tumors extended to this area. Moreover, the interval between 7T and 3T MRI could have allowed changes in tumor edema but was limited to 7 days which reflects clinical routine and minimized the bias. Notably, four patients underwent both MRI examinations on the same day, also showing consistently lower FLAIR-GTVs at 7T. Finally, two patients had received a previous CRT with an interval to MRI of at least 2 months, so that therapy-associated changes were possible but unlikely.

Further limitations of this study include hardware differences as well as slightly varying FLAIR protocols between the different MRI scanners. However, all protocols were optimized with respect to the corresponding hardware. These are the first results from a prospective study investigating high-resolution 7T FLAIR MRI in radiation treatment planning in general and especially for GBM patients. Consequently, our findings form the basis for validations in bigger patient cohorts and investigations of patient outcome following 7T-MRI-based radiotherapy planning.

In conclusion, 7T FLAIR MRI is a clinically feasible imaging technique which could enhance visualization of tumor infiltration as well as neighboring white matter tracts and organs at risk, thus possibly altering treatment planning volumes in radiotherapy.

Conflicts of interest

None.

Acknowledgments

We thank the Dietmar-Hopp-Stiftung for financial support of this work as well as Eric Tonndorf-Martini and Markus Wunderlich for excellent technical assistance. This work has been presented in part at the DEGRO 21.-24.06.2018 in Berlin, Germany.

References

[1] Hajnal JV, De Coene B, Lewis PD, Baudouin CJ, Cowan FM, Pennock JM, et al. High signal regions in normal white matter shown by heavily T2-weighted CSF nulled IR sequences. J Comput Assist Tomogr 1992;16:506–13. Epub 1992/07/01 PubMed PMID: 1629405.

[2] Niyazi M, Brada M, Chalmers AJ, Combs SE, Erridge SC, Fiorentino A, et al. ESTRO-ACROP guideline "target delineation of glioblastomas". Radiother Oncol. 2016;118:35–42. https://doi.org/10.1016/j.radonc.2015.12.003. PubMed PMID: 26777122.

[3] Weller M, van den Bent M, Hopkins K, Tonn JC, Stupp R, Falini A, et al. EANO guideline for the diagnosis and treatment of anaplastic gliomas and glioblastoma. Lancet Oncol 2014;15. https://doi.org/10.1016/s1470-2045(14)70011-7. e395-40. Epub 2014/08/01. PubMed PMID: 25079102.

[4] Cao Y, Tseng CL, Balter JM, Teng F, Parmar HA, Sahgal A. MR-guided radiation therapy: transformative technology and its role in the central nervous system. Neuro Oncol 2017;19:ii16–29. https://doi.org/10.1093/neuonc/nox006. Epub 2017/04/06. PubMed PMID: 28380637; PubMed Central PMCID: PMCPMC5463498.

[5] Stupp R, Mason WP, van den Bent MJ, Weller M, Fisher B, Taphoorn MJ, et al. Radiotherapy plus concomitant and adjuvant temozolomide for glioblastoma. New Engl J Med 2005;352:987–96. https://doi.org/10.1056/NEJMoa043330. Epub 2005/03/11. PubMed PMID: 15758009.

[6] Stupp R, Hegi ME, Mason WP, van den Bent MJ, Taphoorn MJ, Janzer RC, et al. Effects of radiotherapy with concomitant and adjuvant temozolomide versus radiotherapy alone on survival in glioblastoma in a randomised phase III study: 5-year analysis of the EORTC-NCIC trial. Lancet Oncol 2009;10:459–66. https://doi.org/10.1016/s1470-2045(09)70025-7. Epub 2009/03/10. PubMed PMID: 19269895.

[7] Ft Earnest, Kelly PJ, Scheithauer BW, Kall BA, Cascino TL, Ehman RL, et al. Cerebral astrocytomas: histopathologic correlation of MR and CT contrast enhancement with stereotactic biopsy. Radiology 1988;166:823–7. https://doi.org/10.1148/radiology.166.3.2829270. Epub 1988/03/01. PubMed PMID: 2829270.

[8] Halperin EC, Bentel G, Heinz ER, Burger PC. Radiation therapy treatment planning in supratentorial glioblastoma multiforme: an analysis based on post mortem topographic anatomy with CT correlations. Int J Radiat Oncol Biol Phys 1989;17:1347–50. Epub 1989/12/01. PubMed PMID: 2557310.

[9] Demuth T, Berens ME. Molecular mechanisms of glioma cell migration and invasion. J Neurooncol 2004;70:217–28. https://doi.org/10.1007/s11060-004-2751-6. Epub 2005/01/28. PubMed PMID: 15674479.

[10] Kelly PJ, Daumas-Duport C, Kispert DB, Kall BA, Scheithauer BW, Illig JJ. Imaging-based stereotaxic serial biopsies in untreated intracranial glial neoplasms. J Neurosurg 1987;66(6):865–74. Epub 1987/06/01. 10.3171/jns.1987.66.6.0865 PubMed PMID: 3033172.
[11] Vaughan JT, Garwood M, Collins CM, Liu W, DelaBarre L, Adriany G, et al. 7T vs. 4T: RF power, homogeneity, and signal-to-noise comparison in head images. Magn Reson Med 2001;46:24–30. Epub 2001/07/10. PubMed PMID: 11443707.
[12] Ladd ME. High-field-strength magnetic resonance: potential and limits. Top Magnet Resonance Imag TMRI 2007;18:139–52. https://doi.org/10.1097/RMR.0b013e3180f612b3. Epub 2007/07/11. PubMed PMID: 17621228.
[13] Zwanenburg JJ, Hendrikse J, Visser F, Takahara T, Luijten PR. Fluid attenuated inversion recovery (FLAIR) MRI at 7.0 Tesla: comparison with 1.5 and 3.0 Tesla. Eur Radiol 2010;20:915–22. https://doi.org/10.1007/s00330-009-1620-2. Epub 2009/10/06. PubMed PMID: 19802613; PubMed Central PMCID: PMCPMC2835637.
[14] Otazo R, Mueller B, Ugurbil K, Wald L, Posse S. Signal-to-noise ratio and spectral linewidth improvements between 1.5 and 7 Tesla in proton echo-planar spectroscopic imaging. Magn Reson Med 2006;56:1200–10. https://doi.org/10.1002/mrm.21067.
[15] Theysohn JM, Kraff O, Maderwald S, Schlamann MU, de Greiff A, Forsting M, et al. The human hippocampus at 7 T–in vivo MRI. Hippocampus 2009;19:1–7. https://doi.org/10.1002/hipo.20487. Epub 2008/08/30. PubMed PMID: 18727048.
[16] Springer E, Dymerska B, Cardoso PL, Robinson SD, Weisstanner C, Wiest R, et al. Comparison of Routine Brain Imaging at 3 T and 7 T. Investig Radiol 2016;51:469–82. https://doi.org/10.1097/rli.0000000000000256. Epub 2016/02/11. PubMed PMID: 26863580.
[17] Compter I, Peerlings J, Eekers DB, Postma AA, Ivanov D, Wiggins CJ, et al. Technical feasibility of integrating 7 T anatomical MRI in image-guided radiotherapy of glioblastoma: a preparatory study. MAGMA. 2016;29:591–603. https://doi.org/10.1007/s10334-016-0534-7. PubMed PMID: 27026245.
[18] Teeuwisse WM, Brink WM, Haines KN, Webb AG. Simulations of high permittivity materials for 7 T neuroimaging and evaluation of a new barium titanate-based dielectric. Magn Reson Med 2012;67:912–8. https://doi.org/10.1002/mrm.24176. Epub 2012/01/31. PubMed PMID: 22287360.
[19] Hennig J, Scheffler K. Hyperechoes. Magn Reson Med. 2001;46:6–12. Epub 2001/07/10 PubMed PMID: 11443704.
[20] Weigel M, Zaitsev M, Hennig J. Inversion recovery prepared turbo spin echo sequences with reduced SAR using smooth transitions between pseudo steady states. Magn Reson Med 2007;57:631–7. https://doi.org/10.1002/mrm.21170. Epub 2007/02/28. PubMed PMID: 17326168.
[21] Nolden M, Zelzer S, Seitel A, Wald D, Muller M, Franz AM, et al. The Medical Imaging Interaction Toolkit: challenges and advances: 10 years of open-source development. Int J Comput Assist Radiol Surg 2013;8:607–20. https://doi.org/10.1007/s11548-013-0840-8. Epub 2013/04/17. PubMed PMID: 23588509.
[22] Duma CM, Kim BS, Chen PV, Plunkett ME, Mackintosh R, Mathews MS, et al. Upfront boost Gamma Knife "leading-edge" radiosurgery to FLAIR MRI-defined tumor migration pathways in 174 patients with glioblastoma multiforme: a 15-year assessment of a novel therapy. J Neurosurg 2016;125:40–9. https://doi.org/10.3171/2016.7.gks161460. Epub 2016/12/03. PubMed PMID: 27903197.
[23] Gondi V, Hermann BP, Mehta MP, Tome WA. Hippocampal dosimetry predicts neurocognitive function impairment after fractionated stereotactic radiotherapy for benign or low-grade adult brain tumors. Int J Radiat Oncol Biol Phys 2012;83. https://doi.org/10.1016/j.ijrobp.2011.10.021. e487-93. Epub 2012/01/03. PubMed PMID: 22209148; PubMed Central PMCID: PMCPMC3462659.
[24] van den Bent MJ, Carpentier AF, Brandes AA, Sanson M, Taphoorn MJ, Bernsen HJ, et al. Adjuvant procarbazine, lomustine, and vincristine improves progression-free survival but not overall survival in newly diagnosed anaplastic oligodendrogliomas and oligoastrocytomas: a randomized European Organisation for Research and Treatment of Cancer phase III trial. J Clin Oncol 2006;24:2715–22. https://doi.org/10.1200/jco.2005.04.6078. Epub 2006/06/20. PubMed PMID: 16782911.
[25] van den Bent MJ, Brandes AA, Taphoorn MJ, Kros JM, Kouwenhoven MC, Delattre JY, et al. Adjuvant procarbazine, lomustine, and vincristine chemotherapy in newly diagnosed anaplastic oligodendroglioma: long-term follow-up of EORTC brain tumor group study 26951. J Clin Oncol 2013;31:344–50. https://doi.org/10.1200/jco.2012.43.2229. Epub 2012/10/17. PubMed PMID: 23071237.
[26] Cosottini M, Frosini D, Biagi L, Pesaresi I, Costagli M, Tiberi G, et al. Short-term side-effects of brain MR examination at 7 T: a single-centre experience. Eur Radiol 2014;24:1923–8. https://doi.org/10.1007/s00330-014-3177-y. Epub 2014/05/13. PubMed PMID: 24816933.